2024 NDIA MICHIGAN CHAPTER
GROUND VEHICLE SYSTEMS ENGINEERING
AND TECHNOLOGY SYMPOSIUM
POWER AND MOBILITY (PM) TECHNICAL SESSION
AUG. 13-15, 2024 - NOVI, MICHIGAN

EVALUATION OF JETFIRE® PRE-CHAMBER IGNITION FOR LEAN, DI HOMOGENEOUS CHARGE, HEAVY FUELED COMBUSTION AND MULTI-FUEL CAPABILITY

Daniel Nicklowitz[1], Harold Schock[1,2], Thomas Stuecken[1], and Jennifer Higel[2]

[1]Department of Mechanical Engineering, Michigan State University, East Lansing, MI
[2]Mid-Michigan Research, Brighton, MI

ABSTRACT

Michigan State University and Mid-Michigan Research have been studying the potential impact of pre-chamber ignition concepts for nearly two decades. This work demonstrates the performance of a Jetfire® IV system, demonstrating the efficacy of using fuel and air pre-chamber control independent of the primary charge in the main chamber. The invention of the Jetfire® cartridge and cam control system represents a revolutionary change in highly dilute (either with high EGR or very lean) SI engine combustion methodology that has been demonstrated with several fuels, but this work focuses on heavy fuels (JPs), gasoline, and hydrogen. Numerous military applications could benefit from this technology, including drones and other applications where power-dense, fuel-efficient engines are required.

Citation: D. Nicklowitz, H. Schock, T. Stuecken, J. Higel., "Evaluation of Jetfire® Pre-Chamber Ignition for Lean, DI Homogeneous Charge, Heavy Fueled Combustion and Multi-Fuel Capability," In *Proceedings of the 2024 Ground Vehicle Systems Engineering and Technology Symposium (GVSETS)*, NDIA, Novi, MI, Aug. 13-15, 2024 .

1. INTRODUCTION

In recent decades, there has been increasing interest in the development of homogeneous charge, spark-ignited powertrains capable of running on heavy fuel. This interest is largely driven by the US military efforts to employ a "single-fuel strategy," requiring military vehicles and auxiliary power units to operate on JP-5, JP-8, and F-24 fuels [1,2,3]. This strategy was introduced to remedy the logistical challenges of delivering fuel to the battlefield during wartime. Aside from the logistical advantage of requiring all power units to operate on a single fuel, it is desirable for such powertrains to operate on low-volatility, kerosene-based fuels due to safety risks associated with higher-volatility fuels such as gasoline or hydrogen. Kerosene-based

fuels are traditionally well suited for compression ignition (CI) engines due to their low octane number, notable knock propensity, and ignition challenges in spark ignition (SI) configurations. Despite these drawbacks, there are substantial applications for SI engines operating on kerosene-based fuels, notably where high power-to-weight ratios are required or where engine noise is a constraint. Also, many commercially available vehicles such as ATVs, boats etc. are designed to utilize power-dense SI engines. Adaptation of these engine systems to use kerosene-based fuels is the challenge that we have addressed with the Jetfire® system.

Kerosene-based fuels exhibit slow burn rates, significant knock, and poor ignition characteristics in SI engines due to their low octane number, high viscosity, and poor atomization characteristics [4]. These challenges often necessitate a rich air-fuel mixture to promote stable operation and for in-cylinder cooling to mitigate knock [5,6,7]. Operating with excess fuel has obvious disadvantages with respect to fuel efficiency and weight requirements. A high-energy, turbulent jet ignition (TJI) system may help overcome the challenges of slow burn rates and promote reliable ignition.

Pre-chamber ignition systems consist of a small combustion volume in place of a traditional spark plug in an SI engine. The pre-chamber contains a nozzle with several small orifices connecting the pre-chamber volume to the main chamber. The pre-chamber mixture is ignited before the bulk main chamber charge. Shortly after ignition of the pre-chamber, several turbulent jets containing active radicals protrude out of the pre-chamber orifices, subsequently igniting the main chamber bulk charge. These systems are classified as 'active' if they contain a supplementary fuel injection event within the pre-chamber and 'passive' if they contain no supplementary fuel. The turbulent jets provide a substantially higher energy ignition source than traditional SI systems, enabling faster burn rates and reliable ignition of the main chamber charge.

Pre-chamber ignition systems have been shown to improve the lean operating limit of SI engines operating on gasoline, natural gas, and hydrogen fuels [1,8,9]. The active radicals within the turbulent jets provide a high energy ignition source, enabling high dilution rates using either excess air or externally cooled EGR as the diluent. While numerous studies have focused on conventional light-duty fuels, the literature on kerosene-fueled TJI ignition systems is relatively limited. Lui et al. [10] studied the effect of pre-chamber jet ignition (PJI) systems on combustion and knocking characteristics in an SI engine fueled with No. 3 jet fuel. The PJI results were analyzed using a dual spark plug ignition (DSPI) system as a baseline. They found PJI to exhibit a faster rate of heat release (ROHR) than DSPI. Stronger, more consistent combustion was observed using the PJI ignition system as opposed to DSPI, reducing the randomness of knock. Both DSPI and PJI were tested at a 6:1 and 7:1 compression ratio. At the knock limit, PJI exhibited 6.3% lower indicated specific fuel consumption (ISFC) at a compression ratio of 6:1 and 2.1% lower ISFC at a 7:1 compression ratio. For the same ignition timing, PJI had a more significant knock propensity due to the faster rate of heat release and higher peak cylinder pressure.

Other researchers have reported improved knock resistance after implementing a pre-chamber ignition system within a kerosene-fueled engine. Cui et al. [2] found that the knock-limited indicated mean effective pressure (IMEP) could be increased by up to 31.9% by implementing a pre-chamber ignition system in a four-stroke piston aircraft engine fueled with RP3. The increase in IMEP was attributed to the high-energy jets leading to increased flame speed and a higher peak cylinder pressure within the main chamber. The cycle-to-cycle combustion variation was also improved by using a pre-chamber. At low loads and reduced engine speed, the authors noted decreased performance associated with the

pre-chamber. This was attributed to the reduced turbulent kinetic energy within the pre-chamber and higher rates of EGR within the pre-chamber prior to ignition. Additionally, the authors noted overheating issues with larger pre-chamber volume (2.5 mL compared to 1.5 mL). Other researchers have noted ignition challenges relating to exhaust residuals within the pre-chamber [11]. Both of these issues are addressed in the coming discussion.

Wang et al. [4] studied PJI in a Rotax-914 SI engine fueled with aviation kerosene. During this work, the combustion duration was reduced by 20.8% by implementing PJI when operating on kerosene. The authors found PJI to suppress knocking combustion significantly, which was attributed to the faster combustion process. The IMEP under different operating speeds could be increased by 10%-27% when using PJI over traditional SI. Furthermore, the throttle opening could be increased by 42%-66% when using PJI, which can significantly reduce pumping losses.

1.1. Intrduction to Jetfire®

Jetfire® is a pre-chamber process that produces an active turbulent jet controlling the primary combustion chamber process. Compressed scavenge air is delivered via a poppet valve within the pre-chamber, which is actuated shortly before ignition. The scavenge air effectively purges the pre-chamber of exhaust residuals. By controlling the air and fuel directly and independently within the pre-chamber, favorable ignition quality can be maintained within the pre-chamber, even under very lean or EGR-diluted conditions within the main chamber. The initial dual-mode turbulent jet ignition work was sponsored by the US Department of Energy [12]. Subsequent efforts over the past decade resulted in three granted patents [13,14,15] and two pending patents [16,17]. Details of this work are described in several recent reviewed publications [9,18,19].

The differentiating feature of the Jetfire® system is the supplementary scavenge air supplied to the pre-chamber via the poppet ”purge” valve. The supplementary air seeks to address the issue of mixture formation within the pre-chamber and cooling of the nozzle to prevent issues with oxidation and overheating. In traditional pre-chamber systems without supplementary scavenge air, exhaust gas residuals may remain within the pre-chamber from the previous cycle, regardless of the main chamber dilution rate [11]. Residual exhaust gasses within the pre-chamber compromise the mixture ignition quality. By purging the pre-chamber with fresh air before ignition, Jetfire® ensures a fresh mixture within the pre-chamber at ignition. Additionally, the purge air likely helps with fuel atomization within the pre-chamber, possibly eliminating the need for technologies such as air-assisted direct injection to overcome the low volatility and high viscosity of kerosene-based fuels [2,5]. The pre-chamber air may be heated with engine waste heat but was not heated for this study while running kerosene-based fuels. Lastly, the pre-chamber purge air helps keep the nozzle cool, preventing oxidation and overheating of the pre-chamber, an issue encountered by other researchers [2]. After several hundred hours of operation, no issues relating to oxidation of the pre-chamber nozzle have been reported on the Jetfire® system. The pre-chamber, purge valve, spark plug, and fuel injector are packaged within a cartridge assembly, as shown in Figure 1. The pre-chamber events over an engine cycle are summarized in Figure 2

2. EXPERIMENTAL SETUP

This work utilized a single-cylinder test engine configured with the Jetfire® ignition system. The engine clearance volume could vary by utilizing shims beneath the cylinder head. When running kerosene-based fuel, the test engine was configured initially with a 7:1 geometric compression ratio. Two fuels were supplied by the army research lab (ARL), one with a cetane number of 51 (referred to as

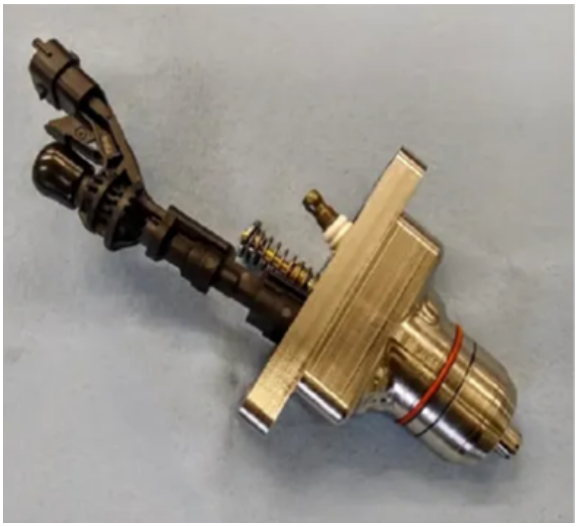

Figure 1: Jetfire® Cartridge

CN50), and the other with a cetane number of 30 (CN30). Both fuels were tested at a compression ratio of 7:1. The CN30 fuel exhibited better knock resistance. Therefore, the CN30 fuel was also tested utilizing an 8:1 geometric compression ratio. Operation with heavy fuels requires a relatively lower compression ratio when compared to traditional SI fuels. This is due to the lower octane number and increased knocking tendency of heavy fuels when compared to fuels such as gasoline. Heavy fuels typically have a lower auto-ignition temperature than traditional SI fuels, allowing them to easily ignite upon injection during CI operation. The objective of this work was to ignite a homogeneous heavy-fueled charge using a pre-chamber rather than through compression. Therefore, a lower compression ratio was required to prevent premature auto-ignition.

The Jetfire® system has also been tested using regular gasoline and hydrogen fuel. These tests occurred at a 15:1 geometric compression ratio. When running gasoline, exhaust gas was sampled and analyzed using a Horiba MEXA 7100 DEGR motor exhaust gas analyzer. The CO2 in the intake was sampled and used along with the CO2 measurement in the exhaust to determine the dilution percentage when running gasoline fuel. Table 1 details the general engine specifications. When operating on heavy fuels or hydrogen, the engine was equipped with DI injection in both the pre-chamber and the main chamber.

Table 1: Major Engine Specifications

Parameter	**Value**
Bore	86.00 mm
Stroke	95.00 mm
Connecting Rod Length	170.00 mm
Compression Ratio	7:1, 8:1, or 15:1
Pre-Chamber Volume	2712 mm^3
Swept Volume	0.552 L
Fuel Injection	100 Bar (Both Chambers)

When operating on gasoline, the main chamber was fueled via high-pressure manifold injection. Cylinder pressure data was acquired using piezoelectric pressure transducers and an A&D Technology Combustion Analysis System (CAS). Pre-chamber pressure data was acquired using a spark plug integrated Kistler pressure transducer (Kistler 6115CF-8CQ01-4-1), while main chamber pressure data was acquired using a separate Kistler (model 6054C) pressure transducer placed within the cylinder head. The ignition energy of the pre-chamber spark plug was approximately 150 mJ. An ECM lambda 5220 wideband lambda sensor was placed in the exhaust to monitor and record the operating air-fuel ratio. A Micro Motion CMFS007M Coriolis flow meter was used to monitor the fuel mass flow rate. The main chamber cylinder pressure data was used to calculate the indicated work and efficiency. Low-speed data, including temperature measurements, flow measurements, etc., were logged at 10 Hz using an in-house LabVIEW-based data acquisition system. Control of the injection, ignition, valve timing, etc., was achieved using an in-house NI Veristand-based control system running a real-time Simulink model. The Veristand system was configured over a

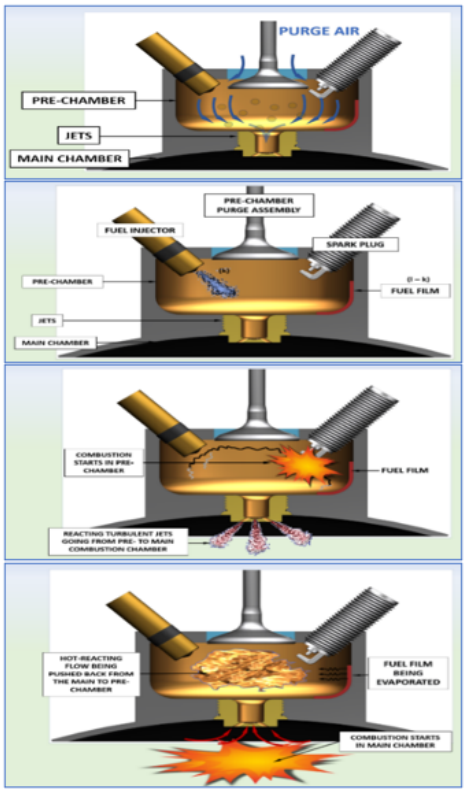

Jetfire® is a Conventional 4-Stroke Cycle Process but with an Advanced Ignition Pre-chamber, Figure 3.

Step 1 of ignition process: During ***Intake****, purge air removes prechamber residuals from previous cycle.*

Step 2: During ***mid-Compression****, fuel in injected into the prechamber, mixed and prepared for spark.*

Step 3. ***Combustion starts inside the pre-chamber*** *leading to the chemically active turbulent jets entering the main combustion chamber.*

Step 4: ***Combustion starts inside the main chamber****, leading to the flow being pushed into the pre-chamber. The hot reacting pushed-back flow causes the pre-chamber fuel film to evaporate.*

Figure 2: Jetfire® Operational Schematic

controller area network (CAN) bus to communicate with three Mototron ECM-5554 controllers, each handling different aspects of the engine control. The engine was coupled to a DC dynamometer to motor the engine when not firing and to absorb the engine torque when firing. Finally, the manifold pressure could be increased via an external electric supercharger for load control. Jetfire® IV utilizes electric cam phasers to independently vary the intake, exhaust, and pre-chamber scavenge valve timing. The intake and purge valves are actuated via a unique concentric camshaft. With this configuration, the intake cam lobes are attached to the outer camshaft, while the purge valve cam lobe is attached to the inner camshaft. Each cam phaser has 70 crank angle degrees of valve timing authority. Figure 3 shows a CAD rendering of the concentric camshaft and the pre-chamber cartridge assembly. Figure 4 shows the engine within the test cell.

2.1. Combustion and Knock Analysis

The indicated mean effective pressure is an important combustion analysis parameter calculated from the cylinder pressure and crankshaft position data. The gross IMEP is calculated as the pressure-volume work during the compression and expansion stroke, normalized by the swept volume. The definition of gross IMEP is provided in Equation (1).

$$IMEP_{gross} = \frac{1}{V_d} \int_{Compression}^{Expansion} P\,dV \qquad (1)$$

Where P is the main chamber pressure, V is the cylinder volume, and V_d is the main chamber displacement volume. Therefore, the gross IMEP is the normalized work done by the combustion gas pressure on the piston crown during the expansion stroke. It is the enclosed area within the ”upper loop”

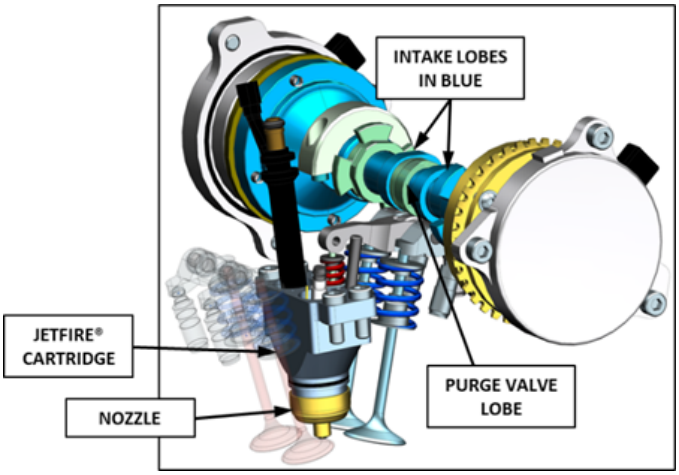

Figure 3: Jetfire® Cylinder Cartridge and Concentric Camshaft

of the pressure-volume curve and does not account for the pumping losses incurred during the intake and exhaust strokes.

Equation (2) represents the IMEP coefficient of variation (COV). The COV is a commonly cited statistical parameter indicating combustion stability.

$$IMEP\,COV(\%) = \frac{\sigma_{\text{IMEP}}}{\mu_{\text{IMEP}}} \cdot 100\% \qquad (2)$$

where σ_{IMEP} is the standard deviation of the IMEP and μ_{IMEP} represents the mean of the IMEP. Each of these quantities is calculated over a moving average statistical window size in real-time while the engine is running. During this work, the statistical window size was 10 cycles. A high COV may indicate partial burning, misfires, or even knocking combustion. It is generally necessary to maintain a COV $< 10\%$.

Knock refers to the undesirable auto-ignition of end gasses beyond the bulk flame front. Knocking combustion exhibits high-frequency pressure oscillations and has the potential to damage engine components. The attributes of knocking combustion can be quantified by high pass filtering ($>$ 4 kHz) the raw cylinder pressure signal, and subtracting the filtered signal from the raw cylinder pressure signal [9]. The resultant signal can be quantified in terms of its amplitude, frequency, etc. Equation

Figure 4: Jetfire® Engine on Test Stand

(3) defines the maximum amplitude of pressure oscillation (MAPO) of the filtered knock trace. This is a commonly cited parameter to quantify the severity of knocking combustion.

$$MAPO = Max|P_{raw} - P_{filtered}| \qquad (3)$$

where P_{raw} is the raw cylinder pressure trace and $P_{filtered}$ is the filtered cylinder pressure trace.

Finally, λ is a commonly referenced combustion parameter representing the ratio of the actual air-fuel ratio to the stoichiometric air-fuel ratio, as described by Equation (4).

$$\lambda = \frac{AFR}{AFR_{\text{stoic}}} \qquad (4)$$

where AFR is the air-fuel ratio measured during the test, and AFR_{stoic} is the stoichiometric air fuel ratio. The stoichiometric air-fuel ratio for gasoline and kerosene-based fuel is approximately 14.70:1. A λ <1 represents a rich mixture, meaning excess fuel

relative to the amount of fresh air. Conversely, $\lambda > 1$ represents a lean mixture containing more oxygen than is necessary to completely oxidize the fuel.

3. RESULTS AND DISCUSSION

3.1. CN30 and CN50 Fuel

Figure 5 summarizes the combustion of the CN30 and CN50 fuels at 1500 RPM and 8.25 bar gross IMEP. The cylinder pressure traces and rate of heat release curves represent the average of 200 cycles, while the maximum amplitude of the pressure oscillation plot shows the data over each of the 200 cycles. It is clear that operation is more knock-limited when running the CN50 fuel, most obviously noting the larger MAPO associated with the CN50 fuel. There also is a higher randomness associated with the MAPO of the CN50 fuel, which is apparent in the larger fluctuations in the MAPO value of the CN50 fuel. The average MAPO over the 200 cycles was 0.72 bar for the CN30 fuel, and 1.83 bar for the CN50 fuel. This more severe knocking tendency indicates a lower peak load capability associated with the CN50 fuel. The cylinder pressure and heat release curves show the more advanced combustion phasing of the CN30 fuel. The point of peak pressure was 14.18 °ATDCF for the CN30 fuel and 26.61 °ATDCF for the CN50 fuel. The delayed combustion is seen in the heat release curve, showing a significant delay in the heat release associated with the CN30 fuel. The delayed combustion of the CN50 fuel is non-optimal and leads to a lower indicated efficiency when compared to the CN30 fuel's more advanced combustion phasing. The ISFC, determined from the gross indicated work and the fuel flow data, was 247.4 $\frac{g}{kW \cdot h}$ while operating on CN30 fuel, and 270.27 $\frac{g}{kW \cdot h}$ while operating on CN50 fuel. When operating on CN50 fuel, the ISFC is approximately 9% higher than when operating on CN30 fuel at this operating condition.

Figure 6 shows the highest load points during the test at various engine speeds. The operation was generally knock-limited at 9 bar $IMEP_{gross}$

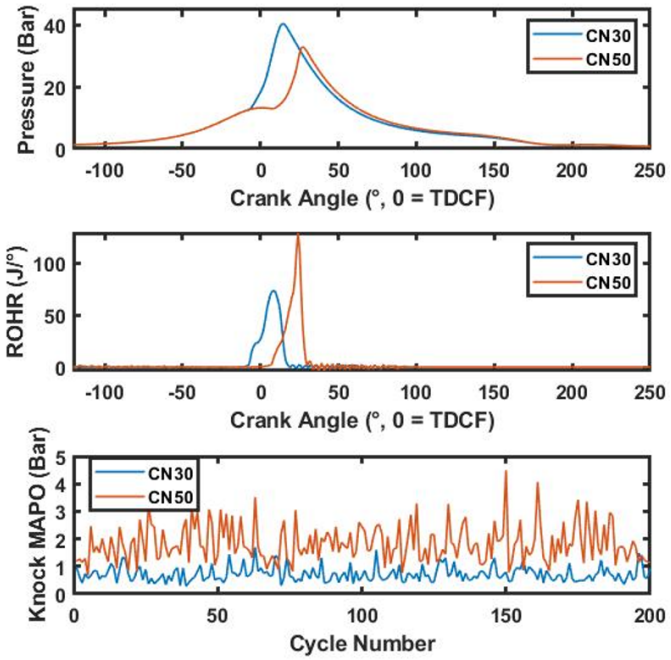

Figure 5: Main Chamber Pressure, ROHR, and MAPO of CN30 and CN50 Fuels at 1500 RPM and 8.25 bar IMEP$_{gross}$

when running on the CN50 fuel. The fueling was increased to λ = 1.0 while using the CN30 fuel, but could only be increased to $\lambda \approx 1.1$ using CN50 fuel due to knock limitations. The maximum load achievable under atmospheric manifold pressure was nominally 10 bar $IMEP_{gross}$, as shown in the CN30 test result. No significant knock limitations were observed with CN30 fuel under atmospheric manifold pressure. The manifold pressure was increased to 1.34 bar absolute to test the load capacity of the engine while running CN30 fuel. This test took place at 4000 RPM. As shown in Figure 6, the maximum load achieved was 13.06 bar $IMEP_{gross}$, corresponding to 24.1 kW indicated power, before the knock exceeded 3 bar MAPO using CN30 fuel.

Figure 7 summarizes the performance by isolating the highest efficiency points at various engine speeds. The CN30 fuel generally exhibits a higher indicated efficiency by 1 to 2 percentage points as a result of the more desirable combustion phasing afforded by the better knock resistance. More extensive testing

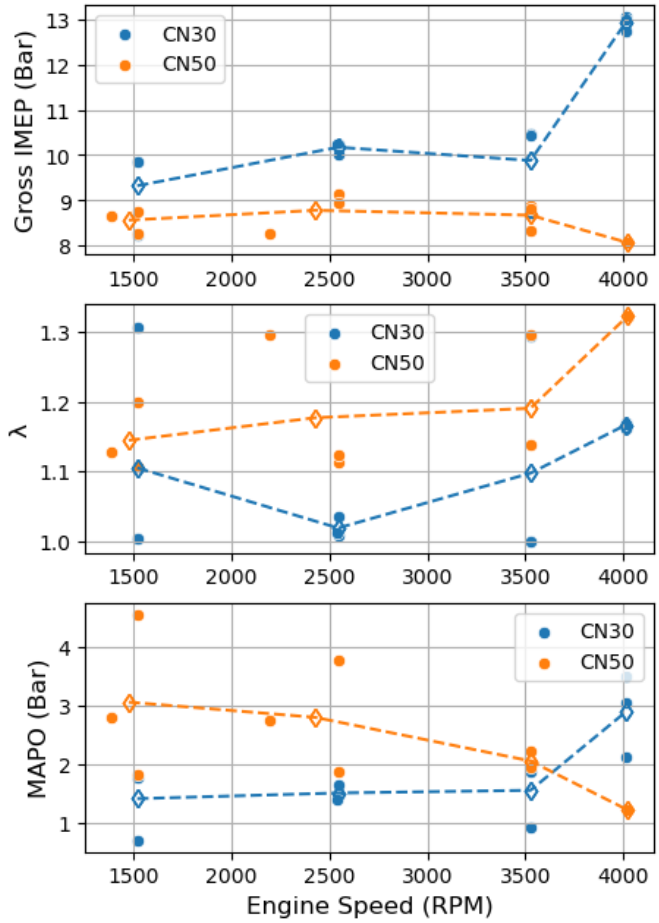

Figure 6: IMEP$_{gross}$, λ, and MAPO of the Maximum Load Points Versus RPM using CN30 and CN50 Fuel

occurred at 2500 RPM using the CN30 fuel, with a maximum λ of 1.79, and the IMEP COV was 4.28%. The highest indicated thermal efficiency measured at a 7:1 compression ratio was 35.88%, corresponding to an ISFC of 230.06 $\frac{g}{kW \cdot h}$ using CN30 fuel. The highest indicated thermal efficiency using CN50 fuel was 34.18%, corresponding to an ISFC of 241.53 $\frac{g}{kW \cdot h}$. The lowest load tested was nominally 2 bar $IMEP_{gross}$ using CN50 fuel, and 2.5 bar $IMEP_{gross}$ using CN30 fuel.

Figure 6 and Figure 7 show stable operation was achieved using both fuels over a range of engine speeds and operating conditions. The performance dip observed with the CN50 fuel relative to the CN30 fuel is expected due to the higher cetane number and associated lower octane number. Given the lower knock resistance, the maximum load tolerance of the higher cetane number fuel is lower than the CN30 fuel. Operation using the CN50 fuel is knock limited in excess of 9 bar gross IMEP, whereas a maximum load of 13 bar was achieved using the CN30 fuel at 4000 RPM. This demonstrates the higher load tolerance of the CN30 fuel.

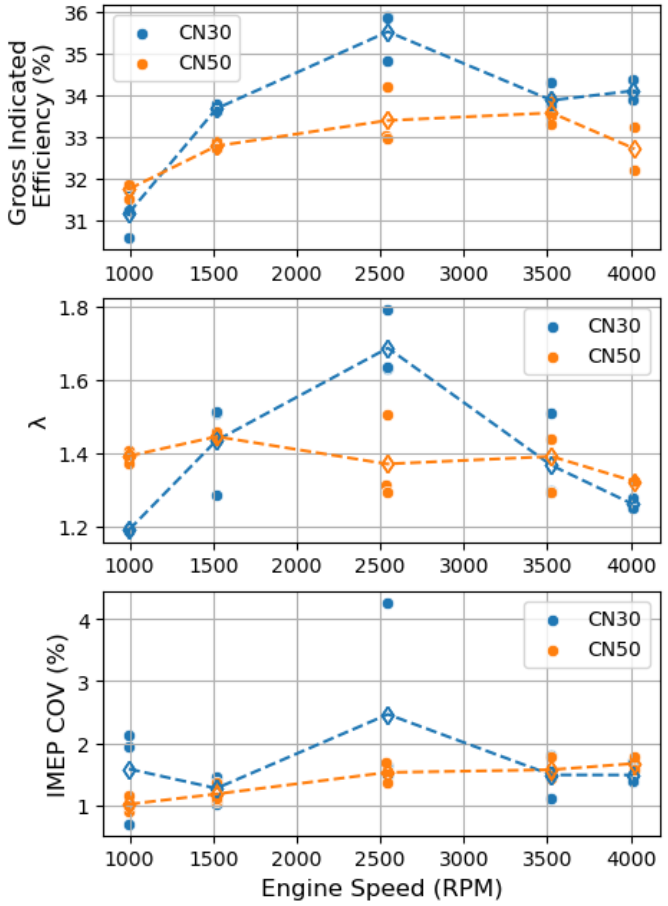

Figure 7: Gross Indicated Efficiency, λ, and $IMEP_{gross}$ COV of the Best Efficiency Points Versus RPM using CN30 and CN50 Fuel

After noting the higher load tolerance of the CN30 fuel, the compression ratio was increased from 7:1 to 8:1 to study the influence of compression ratio on engine performance and knock propensity using CN30 fuel. Testing with the increased

compression ratio occurred at 2500 RPM and was compared to the 7:1 result as a baseline. The fueling was adjusted for both engine configurations to study the lean limit and knock severity near stoichiometric operation. Figure 8 shows the result of the compression ratio comparison over various λ values. Near stoichiometric operation, the 8:1 configuration exhibits a significantly higher knock MAPO than the 7:1 configuration. During testing, 3 bar MAPO has typically been regarded as the acceptable MAPO limit [18]. Secondly, the 8:1 configuration exhibits a more desirable lean burn limit, meaning the fueling can be further reduced while still maintaining stable operation. Under the 8:1 configuration, the fueling could be reduced to $\lambda \approx 2.0$ before exceeding the 3% IMEP COV limit, whereas the fueling could be reduced to $\lambda \approx 1.725$ using the 7:1 configuration. The highest average gross indicated efficiency of 40.36% occured at λ = 1.77 while testing the 8:1 configuration, whereas the highest average efficiency using the 7:1 configuration was 35.3% and occured at λ = 1.66. Most notably, increasing the compression ratio from 7:1 to 8:1 provides nominally a 5 percentage point increase in the maximum indicated thermal efficiency at the expense of a lower knock-limited load tolerance. From the testing at elevated manifold pressure using CN30 fuel, the knock-limited load using the 8:1 configuration is likely 2 to 3 bar lower than the knock-limited load under the 7:1 configuration.

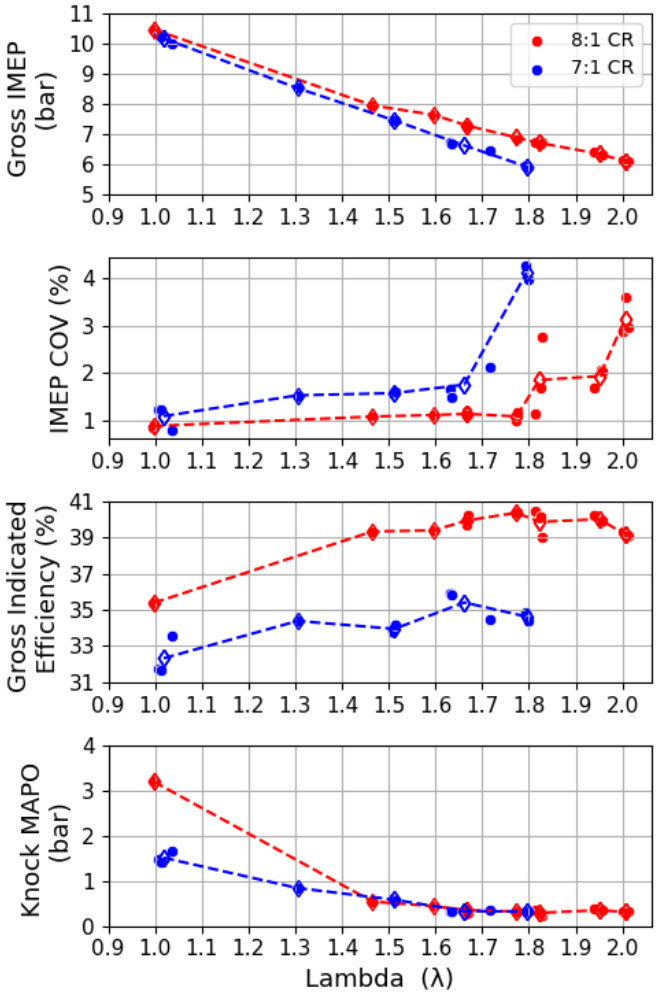

Figure 8: 8:1 vs. 7:1 Compression Ratio Comparison Using CN30 Fuel

3.2. Gasoline

The Jetfire® TJI system has also been tested with gasoline fuel under lean and highly diluted conditions using externally cooled EGR as the diluent [9,18]. Jetfire® is particularly well suited for highly diluted operation using externally cooled EGR. The scavenge valve within the pre-chamber enables very effective pre-chamber purging at relatively low scavenge air pressure compared to other TJI systems utilizing pre-mixed air and fuel injection or separate fuel and air injectors. The high scavenge air flow rate allows the pre-chamber to maintain favorable mixture quality for ignition even at high main chamber dilution rates. Using cooled EGR as the diluent rather than excess air allows for reduced fueling while still maintaining stoichiometric operation, enabling a standard three-way catalyst after-treatment system. Using EGR as a diluent also significantly lowers the combustion temperature, reducing in-cylinder heat losses and NOx formation. A drawback of EGR dilution is increased hydrocarbon emissions due to a reduction in combustion efficiency.

The following discussion details Jetfire®

Generation IV TJI system testing using AKI 87 octane, EPA Tier III gasoline under various EGR dilution rates. The dilution percentage is calculated according to equation 5 by sampling the CO2 in the intake and exhaust gasses using the Horiba emissions bench [9].

$$\text{EGR Volume } (\%) = \frac{CO_{2(intake)}}{CO_{2(exhaust)}} \cdot 100\% \qquad (5)$$

A 15:1 geometric compression ratio was utilized while testing with gasoline. The following results represent a single operating speed of 2750 RPM over various engine loading conditions and EGR dilution rates. EGR sweeps were carried out at 5, 7, 9, and 11 bar gross IMEP. Figure 9 details the gross indicated efficiency and IMEP COV versus EGR dilution percentage at the various loading conditions. Very stable operation, with an IMEP COV $< 3\%$, was maintained up to 40% EGR at 5, 7, and 9 bar IMEP. At 11 bar IMEP, the dilution tolerance was significantly reduced from the lower loading conditions. The EGR dilution could be increased to approximately 32.5% before exceeding 3% IMEP COV. At 11 bar gross IMEP, the spark could not be advanced to maximum brake torque (MBT) timing due to knock. The more delayed ignition timing and associated higher main chamber cylinder pressure at the point of ignition likely force residuals back into the pre-chamber, compromising the ignition quality. Furthermore, EGR dilution significantly slows the burn rate of the bulk charge. The slow burn rate combined with the late ignition timing may cause the bulk flame front to extinguish prematurely, further contributing to the lower dilution tolerance. The maximum indicated thermal efficiency of 48.16% occured at 9 bar gross IMEP and nominally 37% EGR dilution. The maximum thermal efficiency at 5, 7 and 11 bar IMEP were 45.29%, 47.27%, and 46.56%, respectively. Dilution rates beyond the peak efficiency point resulted in lower combustion stability and reduced overall efficiency. The reduced combustion stability is revealed through the sharply increasing IMEP COV beyond the 40% EGR at 5, 7, and 9 bar gross IMEP, and beyond 32.5% EGR at 11 bar gross IMEP.

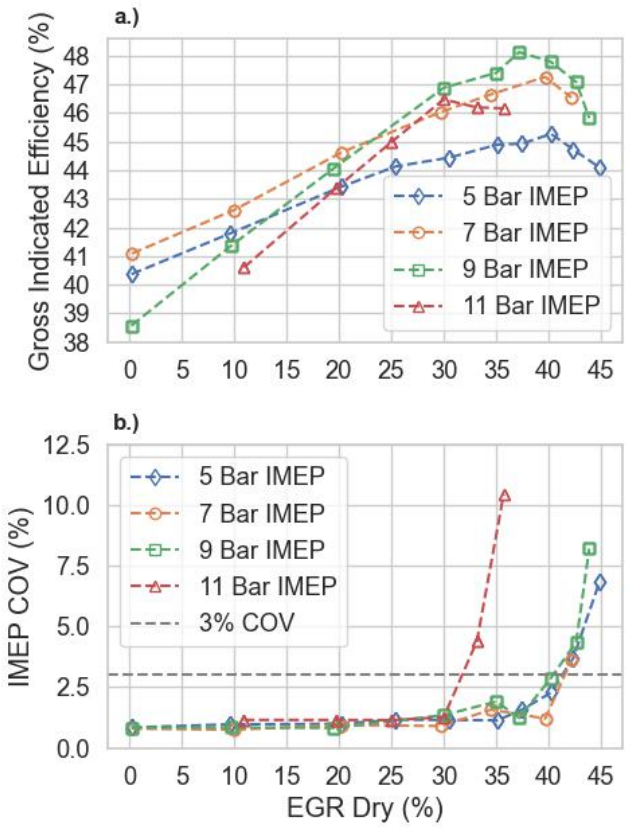

Figure 9: Efficiency and IMEP COV vs EGR Dilution Using EPA Teir III Gasoline, 15:1 CR, 2750 RPM

Figure 10 illustrates a breakdown of the energy losses and indicated work at 9 bar gross IMEP. Three dilution rates are shown to describe the effect of EGR dilution on the various losses and the associated gain in the indicated work. The net indicated work is calculated from the in-cylinder pressure data and does not account for the pumping losses. The pumping losses are a separate term within the energy balance and are also calculated from the in-cylinder pressure data. The exhaust heat loss is calculated from the air flow rate and temperature data, and

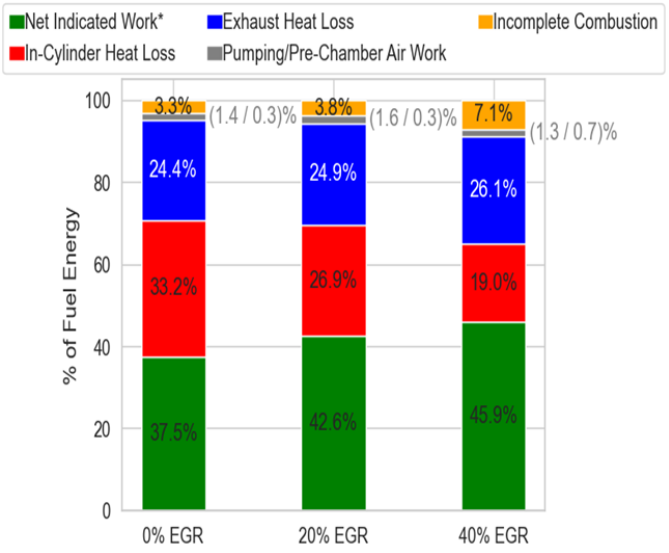

Figure 10: In Cylinder Energy Balance at 0%, 20%, and 40% EGR Dilution using Gasoline Fuel

the incomplete combustion is calculated from the exhaust gas composition data. The work required to deliver the pre-chamber air is calculated following a Womack Fluid Power Design data sheet, which assumes a single-stage compressor with an 85% isentropic efficiency [24]. The in-cylinder heat loss is calculated by subtracting the losses and the net indicated work from the total fuel energy. A very important result is the minimal loss associated with the pre-chamber scavenge air delivery. Across the dilution range, the work required to deliver the pre-chamber scavenge air results in a 0.3% to 0.7% reduction in thermal efficiency, depending on the operating condition. Higher dilution rates generally require an increase in pre-chamber scavenge air pressure, which significantly affects the energy loss associated with scavenge air delivery. The energy balance in Figure 10 also shows a dramatic reduction in the in-cylinder heat loss associated with EGR dilution. This is a result of the lower in-cylinder combustion temperatures with increasing dilution rate. There is an increase in the exhaust heat loss percentage, which can be attributed to the slower burn rate associated with high EGR dilution. There is also an increase in incomplete combustion energy loss at the high EGR dilution rates, which is a result of the reduced combustion efficiency associated with EGR dilution. Overall, there is a significant gain in the net indicated work percentage, which is primarily driven by the reduced in-cylinder heat loss as a result of lower combustion temperature at high EGR dilution rates.

Figure 11 shows the reduction in NOx emissions and increase in hydrocarbon emissions associated with EGR dilution. The maximum NOx emissions of 3350 ppm occur at 0% EGR dilution. The minimum measured NOx emissions were 51 ppm and occured at nominally 42.5% EGR dilution. This represents a 98% reduction in NOx from the maximum to the minimum value. At the peak efficiency operating

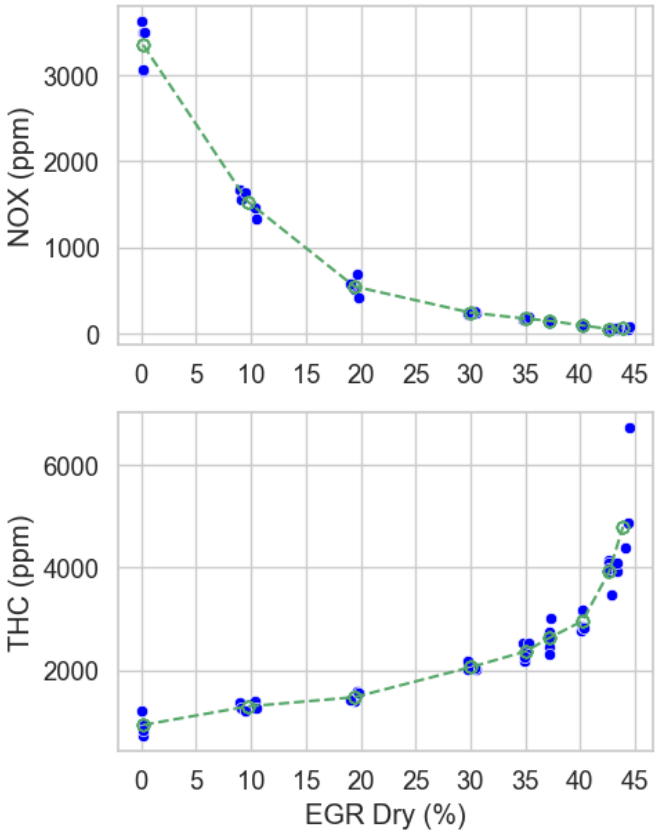

Figure 11: NOx and THC Emissions vs EGR Dilution, 9 bar IMEP Gasoline Fuel

point, the NOx emission concentration was 147 ppm, corresponding to 0.69 indicated $\frac{g}{kW \cdot h}$. The reduction in NOx emissions comes at the expense of increased hydrocarbon emissions, also shown in Figure 11. This is a potential area of future research. The combustion efficiency associated with the highest indicated efficiency was nominally 94%. If the combustion efficiency could be improved through CFD optimization of the pre-chamber, it would increase the indicated efficiency and reduce the hydrocarbon emissions.

3.3. Hydrogen

The Jetfire® IV TJI system has been demonstrated using compressed hydrogen as the fuel source using the 15:1 compression ratio configuration. The engine remained largely unmodified from the gasoline testing with the exception of a few changes. A crankcase ventilation port was installed to avoid a buildup of combustion gasses in the crankcase. A remote fuel shutoff valve and solenoid were configured to allow the fuel supply to be cut off from the control room without having to enter the test cell. The external supercharger was also removed from the setup, and the intake manifold was exposed to the atmosphere instead. This eliminated the potential for boosting and removed the EGR circuit. Testing occurred at relatively low loads. A direct measurement of the fuel mass flow was not acquired during the hydrogen testing. Instead, experiments were conducted by firing the injector into a graduated cylinder with a bubble membrane to estimate the flow rate. This experiment provided an initial estimate of the hydrogen flow rate for a given injection pressure and pulse duration.

Figure 12 shows the IMEP COV versus IMEP over various engine speeds using hydrogen as fuel. Extremely stable operation, with a COV $<1\%$, could be maintained at loads greater than 3.5 bar gross IMEP. No significant knocking was observed over the range of operation tested.

Pressure oscillations up to approximately 4 bar

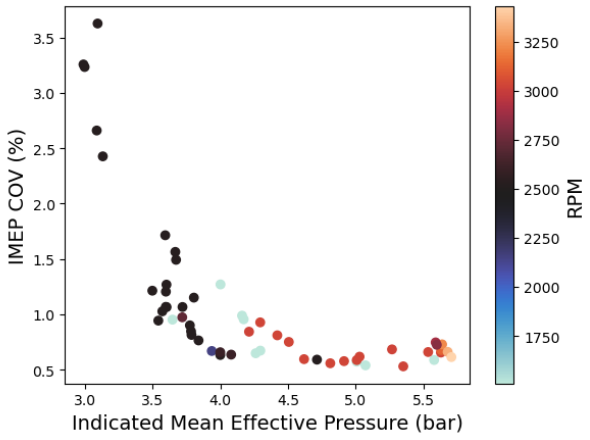

Figure 12: IMEPg COV Vs IMEP Using Hydrogen Fuel

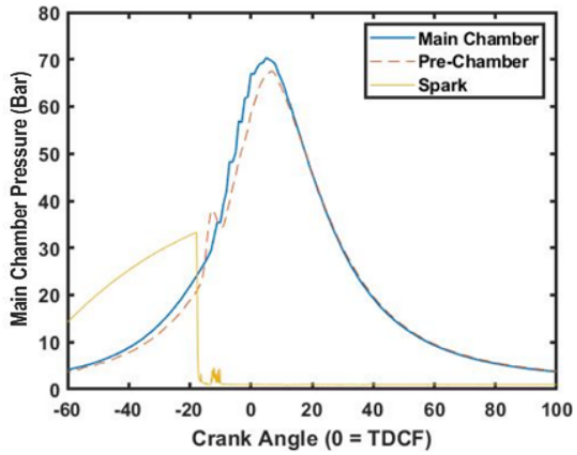

Figure 13: Pressure Oscillations Using Hydrogen Fuel

were observed just after ignition but before the point of maximum cylinder pressure. This effect is shown in the pressure trace of Figure 13. Other researchers of TJI systems have also reported this phenomenon and have attributed the pressure oscillations to the rapid burning of the bulk charge rather than end gas auto-ignition [9,20,21,22,23]. Therefore, the pressure oscillations observed just after ignition are not classified as knocking combustion.

Figure 14 shows the estimated indicated efficiency versus gross IMEP at various engine speeds. The estimate was obtained using the fuel flow rate from

the injector flow rate experiment described above. This strategy yields estimated thermal efficiencies up to 49% at 4.2 bar gross IMEP. While the preliminary results are promising, direct measurement of fuel mass flow during engine operation is needed to validate the efficiency prediction. If validated, the results suggest thermal efficiencies approaching or exceeding 50% may be achievable.

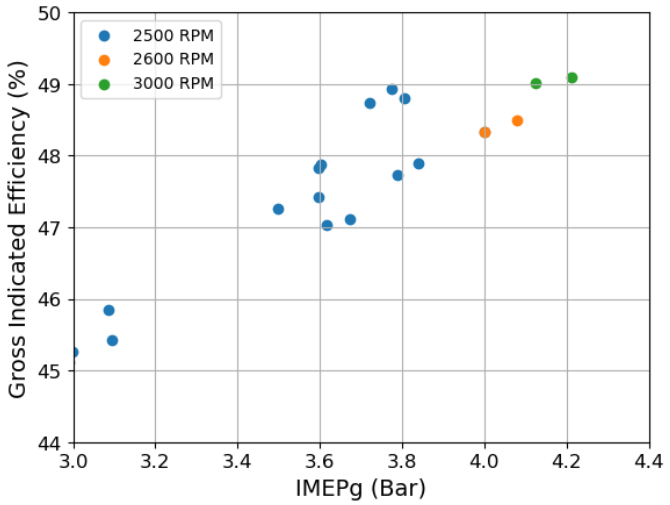

Figure 14: $IMEP_{\text{gross}}$ Vs. Gross Indicated Efficiency Using Hydrogen Fuel

4. CONCLUSIONS AND FUTURE WORK

This work evaluated Jetfire® Turbulent Jet Ignition (TJI) for use with kerosene-based fuels, AKI 87 gasoline, and hydrogen. All testing occured at steady state operation, and the results demonstrate the versatility and robustness of the Jetfire® TJI system for use with various fuel sources. The results are summarized by fuel source below.

4.1. CN30 and CN50 Kerosene

- At a 7:1 compression ratio, CN50 fuel was knock limited in excess of 9 bar gross IMEP across the RPM range, while CN30 fuel could achieve nominally 13 bar gross IMEP under elevated manifold pressure before exceeding the knock MAPO 3 bar limit.
- Both fuels achieve very stable operation from 1000 RPM to 4000 RPM and a range of loading conditions.
- The CN30 fuel was evaluated at a 7:1 compression ratio and an 8:1 compression ratio. Increasing the compression ratio yields a 2 to 3 bar reduction in the maximum tolerable load, but nominally a 5% improvement in the maximum thermal efficiency.

4.2. AKI 87 Gasoline

- Jetfire® IV achieved a maximum dilution tolerance of 40% externally cooled EGR by volume at 5, 7, and 9 bar gross IMEP. The maximum dilution tolerance at 11 bar gross IMEP was nominally 32.5% due to the delayed knock-limited spark advance.
- The maximum indicated thermal efficiency of 48.16% occurred at nominally 37% EGR dilution.
- The work required to deliver pre-chamber scavenge air results in a 0.3% to 0.7% reduction in overall thermal efficiency.
- NOx may be reduced by up to 98% from the 0% dilution condition, but at the expense of increasing hydrocarbon emissions.

4.3. Hydrogen

- Jetfire® IV achieves extremely stable operation with a COV $<1\%$ with gross IMEP between 3.5 and 5.8 bar.
- Estimated indicated thermal efficiencies as high as 49% were achieved with hydrogen fuel. Direct measurement of the fuel flow rate during operation is required to validate the efficiency.
- Pressure oscillations up to 4 bar were observed just after ignition, but prior to the point of peak cylinder pressure while running

hydrogen. These oscillations were not classified as knocking combustion; rather, they were attributed to the rapid burning of the bulk charge associated with the turbulent jets.

There is great potential for future work on evaluating the Jetfire® TJI system for use in several specific applications. Cold start is a significant issue for use with kerosene-based fuels. The engine was pre-heated before testing for this study. There is the potential for only heating the pre-chamber to address cold start. A study should evaluate the cold-start performance of the Jetfire® system using heavy fuels. This study should address strategies such as pre-heating the pre-chamber to improve cold start performance.

A performance reduction was observed when operating with the higher cetane (CN50) fuel as compared to the CN30 fuel. Certain sustainable aviation fuels, such as hydroprocessed esters and fatty acids (HEFA) fuels, may have a significantly higher cetane number than the fuels tested during this study. Higher cetane fuels are expected to exhibit a lower maximum knock-limited load tolerance based on the trends observed with the two tested fuels. This may be addressed through knock suppression strategies such as cooled exhaust gas recirculation, over-fueling or water injection during high-load operation, etc. Future efforts should assess the feasibility of higher cetane number fuels and various knock suppression strategies.

Regarding use with gasoline, transient operation remains mostly unexplored pertaining to TJI systems with high EGR dilution rates. A study should be conducted to assess the feasibility of achieving simultaneous high-efficiency operation and acceptable transient performance. Furthermore, a CFD optimization study on the pre-chamber may improve combustion efficiency and reduce hydrocarbon emissions.

Lastly, the efficiency results need to be validated and elaborated on for use with hydrogen fuel. Direct measurement of the hydrogen fuel flow rate is required during operation. Higher loads should be tested to quantify the knock limitations while running hydrogen fuels, possibly at various compression ratios.

5. ACKNOWLEDGEMENTS

Much of this work has been supported by the US Army, Ground Vehicle Systems Center, Warren Michigan. The authors wish to thank the DEVCOM GVSC group for their intellectual and financial contributions.

6. REFERENCES

[1] B. Wang, F. Xie, W. Hong, J. Du, H. Chen, and X. Li, “Extending ultra-lean burn performance of high compression ratio pre-chamber jet ignition engines based on injection strategy and optimized structure,” Energy, vol. 282, p. 128433, Nov. 2023, doi: 10.1016/j.energy.2023.128433.

[2] H. Cui, Z. Zhao, F. Zhang, C. Yu, and L. Wang, “Effect of pre-chamber volume on combustion characteristics of an SI aircraft piston engine fueled with RP3,” Fuel, vol. 286, p. 119238, Feb. 2021, doi: 10.1016/j.fuel.2020.119238.

[3] W. P. Attard, H. Blaxill, E. K. Anderson, and P. Litke, “Knock Limit Extension with a Gasoline Fueled Pre-Chamber Jet Igniter in a Modern Vehicle Powertrain,” SAE Int. J. Engines, vol. 5, no. 3, pp. 1201–1215, Apr. 2012, doi: 10.4271/2012-01-1143.

[4] L. Wang, Z. Zhao, C. Yu, and H. Cui, “Experimental study of aviation kerosene engine with PJI system,” Energy, vol. 248, p. 123590, Jun. 2022, doi: 10.1016/j.energy.2022.123590.

[5] Z. Chen, B. Liao, Y. Yu, and T. Qin, “Effect of equivalence ratio on spark ignition combustion of an air-assisted direct injection heavy-fuel two-stroke engine,” Fuel, vol. 313, p. 122646, Apr. 2022, doi: 10.1016/j.fuel.2021.122646.

[6] C. Hu, Z. Zhang, M. Tian, N. Liu, and S. Wei, "Research on application of asymmetrical Pre-chamber in Air-Assisted direct injection kerosene engine," Applied Thermal Engineering, vol. 204, p. 117919, Mar. 2022, doi: 10.1016/j.applthermaleng.2021.117919

[7] B. Beyfuss et al., "Evaluation of Spark-Ignited Kerosene Operation in a Wankel Rotary Engine," presented at the Automotive Technical Papers, May 2021, pp. 2021-01–5046. doi: 10.4271/2021-01-5046.

[8] S. Biswas and L. Qiao, "Ignition of ultra-lean premixed H2/air using multiple hot turbulent jets generated by pre-chamber combustion," Applied Thermal Engineering, vol. 132, pp. 102–114, Mar. 2018, doi: 10.1016/j.applthermaleng.2017.11.073.

[9] C. A. A. Atis, Y. Ayele, T. Stuecken, and H. Schock, "Effect of pre-chamber scavenging strategy on EGR tolerance and thermal efficiency of pre-chamber turbulent jet ignition systems," International Journal of Engine Research, vol. 24, no. 5, pp. 1938–1960, May 2023, doi: 10.1177/14680874221105162.

[10] F. Liu, L. Zhou, J. Hua, C. Liu, and H. Wei, "Effects of pre-chamber jet ignition on knock and combustion characteristics in a spark ignition engine fueled with kerosene," Fuel, vol. 293, p. 120278, Jun. 2021, doi: 10.1016/j.fuel.2021.120278

[11] R. Rajasegar, A. Srna, R. Novella, and I. Barbery, "Exploring the EGR Dilution Limits of a Pre-Chamber Ignited Heavy-Duty Natural Gas Engine Operated at Stoichiometric Conditions - An Optical Study," presented at the WCX SAE World Congress Experience, Detroit, Michigan, United States, Apr. 2023, pp. 2023-01–0256. doi: 10.4271/2023-01-0256.

[12] NSF/DOE Grant CBET-1258581, "NSF/DOE Partnership on Advanced Combustion Engines-Modeling and Experimental Studies of Controllable Cavity Turbulent Jet Ignition Systems," 09/15/2013-08/31/2016 (Toulson, Schock, Zhu, Jaberi, Brereton, Wichman)

[13] Schock, H., Zhu, G., Toulson, E., Stuecken, T. Internal Combustion Engine (December 25, 2018). U.S. Patent No. US 10,161,296 B2. East Lansing, MI: U.S. Patent and Trademark Office.

[14] Schock, H and Zhu, G. "Diesel Engine with Turbulent Jet Ignition," US Patent 11,187,142 B2 Nov. 30, 2021

[15] Schock, H. and Stuecken, T., "Engine Turbulent Jet Ignition System," US Patent 11,408,329 B2, Aug. 8, 2022

[16] Schock, H., "Internal Combustion Engine Including Multiple Fuel Injections External to the Pre-Chamber," Submitted to USPTO 5/20/2020, patent pending.

[17] Schock, H., Stuecken, T., Higel, J., and Hunter, G., "An Actuation System for an Internal Combustion Engine," Submitted to the USPTO 7/30,22, patent pending.

[18] Atis, C. (2021). HIGH-EGR DILUTION ENABLED BY DUAL MODE, TURBULENT JET IGNITION (DM-TJI) FOR HIGH-EFFICIENCY INTERNAL COMBUSTION ENGINES [Doctoral Dissertation, Michigan State University].

[19] Vedula, R., Song, R., Stuecken, T. Zhu G., and Schock, H., "Thermal Efficiency of a Dual-Mode TJI Engine under Lean and Near-Stoichiometric Operation," Int. J. of Engine Res., 18(10):1055-1066, 2017

[20] Sens M and Binder E. Pre-chamber ignition as a key technology for future powertrain fleets. MTZ Worldw 2019; 80(2): 44–51.

[21] Yu X, Zhang A, Baur A, Voice A and Engineer N. Statistical quantification of knock with spark ignition and pre-chamber jet ignition in a light duty gasoline engine. In: Proceedings of the ASME 2020 internal combustion engine division fall technical conference, 2020, pp.1–21. DOI: 10.1115/ICEF2020-2941.

[22] Hua J, Zhou L, Gao Q and Feng Z. Effects on cycle-to-cycle variations and knocking combustion of turbulent jet ignition (TJI) with a small volume pre-chamber. SAE technical paper 2020–April, 2020, pp.1–13. DOI: 10.4271/2020-01-1119.

[23] Hokimoto S, Kuboyama T, Moriyoshi Y and Yamada T. Combustion analysis in a natural gas engine with prechamber by three-dimensional numerical simulation. Trans JSME 2015; 81(830): 15–00154.

[24] Womack Machine Supply Co. ”Horsepower Required for Compressing Air,” www.womackmachine.com/engineering-toolbox/data-sheets/horsepower-required-for-compressing-air/ (accessed 6 June 2024).